Journal of Statistical Physics, Vol. 93, Nos. 3/4, 1998

Characterization of Labyrinthine Patterns and Their Evolution

Ronald E. Jones[1] and Gemunu H. Gunaratne[1,2]

Received December 8, 1997

An invariant measure δ is introduced to quantify the disorder in extended locally striped patterns. It is invariant under Euclidean motions of the pattern, and vanishes for a uniform array of stripes. Irregularities such as point defects and domain walls make nonzero contributions to the measure. The evolution of random initial states to labyrinthine patterns is analyzed through the time evolution of δ. This behavior is configuration independent, and exhibits two phases each with a logarithmic decay in δ.

KEY WORDS: Spatiotemporal patterns; labyrinthine patterns; Euclidean symmetries; Gray–Scott model.

1. INTRODUCTION

Nature abounds with spatio-temporal patterns ranging from cloud formation and patterns in sand dunes, to animal coats, fish scales and beehives.[1] The patterns are regular on a small scale (typically consisting of stripes or hexagons) but form highly complex structures on a large scale. The nonlinearity of the underlying systems implies that the details of patterns depend sensitively on the initial conditions. The two patterns shown in Fig. 1 are obtained by evolving two distinct sets of random initial states through the Gray–Scott equations[2] used to model a simple reaction-diffusion system. The patterns are clearly different in detail, but appear to share similar characteristics, such as domain size and defect densities.

The first aim of a theoretical analysis of labyrinthine patterns should be the identification of suitable characterizations; in particular patterns generated under identical control parameters (and visually similar) should

[1] Department of Physics, University of Houston, Houston, Texas 77204.
[2] Institute of Fundamental Studies, Kandy, Sri Lanka.

0022-4715/98/1100-0427$15.00/0

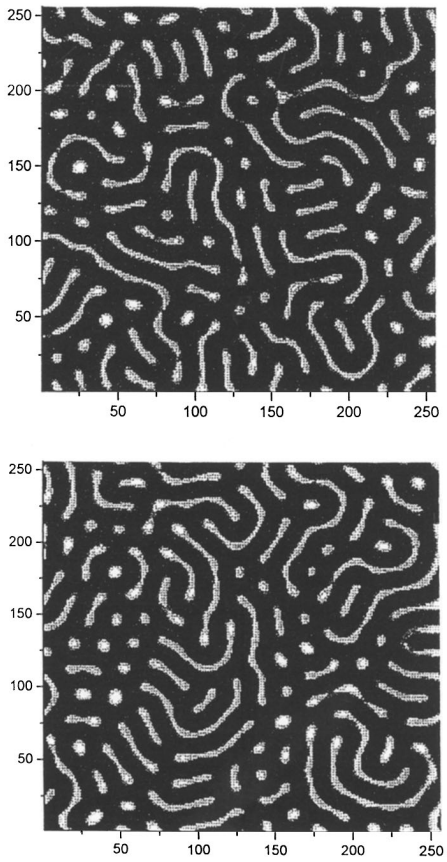

Fig. 1. Two patterns generated by evolving random initial states via the Gray–Scott model for 32,000 time units. Although the patterns are different in detail, it is easy to discern common characteristics between them.

be assigned the same set of measures. The characterizations should also be capable of contrasting visually different patterns. Such an identification would be analogous to the determination of "ensemble independent" variables (e.g., pressure, entropy) in statistical mechanics, or the deduction of dynamical invariants (e.g., fractal dimension, Lyapunov exponent) in chaotic systems.[3]

Most characterizations introduced for this purpose, thus far, were "borrowed" either from Statistical Mechanics or Dynamical Systems Theory. They include Correlation Length,[4,5] Spectral Entropy,[6] spherically averaged Structure Factor,[7] and Lyapunov Dimension Density.[8] None of the measures make explicit use of the local (striped) nature of the

patterns; consequently, their estimation requires the analysis of large data sets. The methods are also not strictly applicable in the presence of the continuous rotational symmetry. For example, these methods fail to provide a reasonable characterization of target patterns.

In this paper we introduce a characterization, referred to as the disorder parameter δ,[9] of labyrinthine patterns that is evaluated from an underlying scalar field $U(\mathbf{x})$. The observed organization of patterns can be quantified using the dynamics of δ. Even though multiple runs of the (numerical) experiments give patterns that are very different in detail, δ captures *configuration independent* features of the relaxation of the patterns to their apparent equilibrium.

In Section 2 we introduce the *envelope function* of a striped pattern and discuss the advantages of using it to describe a labyrinthine pattern. It is impossible to compare distinct configurations generated under fixed external conditions (such as those of Fig. 1) due to the absence of an analytical form for the fields. We instead require that the characterizations be equivariant[10] under all *rigid motions* of a given pattern. In Section 2, we use a representations of the group actions to determine the form of a local measure suitable to quantify deviations of the patterns from perfect stripes. The analysis leads to the definition of the disorder parameter δ.

In Section 3 we present calculations of δ for several patterns with known analytical forms. These results are used to check the accuracy of the numerical methods introduced in Section 4, and to point out several desirable features of δ. The evolution of patterns from the Gray–Scott model[2] is presented in Section 5, and it is shown that δ captures certain *configuration independent* (but parameter dependent) aspects of the relaxation of initially random states to their final configurations. In the concluding section we discuss how the analysis can be extended to study experimental patterns.

2. THE DISORDER PARAMETER

Since the patterns under consideration are locally striped, it is desirable to expand the field $U(\mathbf{x})$ as

$$U(\mathbf{x}) = A(\mathbf{x})\, e^{i\mathbf{k}\cdot\mathbf{x}} + c.c. \tag{1}$$

where the complex field $A(\mathbf{x})$ is the *envelope function*.[11] The magnitude of $\mathbf{k}$ is $k_0 = 2\pi/\lambda$, λ being the characteristic wavelength of the pattern. The addition of the complex conjugate *c.c.* allows the field $U(\mathbf{x})$ to be real. Since the basic state $e^{i\mathbf{k}\cdot\mathbf{x}}$ is factored out of $U(\mathbf{x})$, the envelope function varies on

a scale large compared with λ. Consequently the expansion (1) can also be used to reduce the experimental noise, through suitable local averaging.

The characterizations that we introduce are required to quantify the deviations of a pattern from a *perfect* array of stripes; i.e., an array of stripes with a fixed width pointing in a fixed direction everywhere. We state the minimum requirements for such measures.

2.1. Requirements

A suitable measure δ of the disorder of patterns should satisfy the following criteria:

1. δ must record local deviations of the pattern from stripes (with a given wave vector k_0). Any such deviation should increase δ. The variations in the envelope function $A(\mathbf{x}, t)$ in terms of an operator $\odot$ (to be defined) captures these variations.

2. Analytical representations of a labyrinthine pattern are not available; hence the evaluation of δ needs to be done by estimating derivatives of the field $A(\mathbf{x})$ using values given on a grid. Thus δ should not include higher-order derivatives. (For a few simples types of patterns we are able to evaluate δ analytically. They will be used to calibrate the errors in the numerical algorithms.)

3. Every deviation of the pattern from a perfect set of stripes should increase our measurement. We want our measure to notice domain walls, dislocations, or an instabilities such as variations of wavelength or curvature of contour lines.

4. For complex labyrinthine patterns, δ should be extensive. A corresponding intensive variable $\bar{\delta} = \delta/Area$ can be used to compare the disorder in distinct classes of patterns.

5. δ needs to be invariant under Euclidean transformations. Since rotating, relocating, and flipping the pattern do not change the pattern itself, any sensible measurement of disorder should not change under these transformations either.

2.2. Group Structure

The Euclidean group in two dimensions contains translations, reflections, and rotations This group is written as $O(2) + \Re^2$ where $O(2)$ is the group of rotations and reflections in two dimensions and $\Re^2$ is an ordered pair of real numbers representing the translational group in two dimensions. Given the functional form of a pattern, we can deduce that of a second pattern related by a rigid motion.

Since analytical forms of the fields representing our patterns are not available, it is a priori impossible to determine the form of δ that will capture the common features of distinct configurations generated under identical conditions. We instead require that δ be invariant under all rigid motions of a single structure. As shown below these invariances provide possible terms of the measure δ.

Suppose a pattern $U(\mathbf{x})$ undergoes a rigid action γ. The value of the new field $U'(\mathbf{x}')$ at $\mathbf{x}'$ is the same as that of $U(\mathbf{x})$ at $\mathbf{x} = \gamma^{-1}\mathbf{x}'$.

$$U(\mathbf{x}) = U'(\mathbf{x}') = U'(\gamma\mathbf{x}) \tag{2}$$

By enforcing equivariance under Euclidean motion on the patterns, we can determine the relationship between the envelopes.

(a) Translation. For a translation, γ_T: $\mathbf{x} \to \mathbf{x}' = \mathbf{x} + \mathbf{x}_t$. The pattern $U'(\mathbf{x}')$ is written using Eq. (1) as

$$\begin{aligned} U'(\mathbf{x}') &= A'(\mathbf{x}')\, e^{i\mathbf{k}\cdot\mathbf{x}'} + A'^*(\mathbf{x}')\, e^{-i\mathbf{k}\cdot\mathbf{x}'} \\ &= A'(\mathbf{x}')\, e^{i\mathbf{k}\cdot(\mathbf{x}-\mathbf{x}_t)} + A'^*(\mathbf{x}')\, e^{-i\mathbf{k}\cdot(\mathbf{x}-\mathbf{x}_t)} \end{aligned}$$

Using the equivariance (Eq. (2)),

$$A'(\mathbf{x}') = A(\mathbf{x})\, e^{i\mathbf{k}\cdot\mathbf{x}_t} \tag{3}$$

Thus, translating a pattern introduces a constant phase shift in the envelope.

(b) Reflection. Reflections flip the pattern about an axis in the plane of the pattern. The group action is $\gamma_K \in K$: $\gamma_K(x, y) \to (-x', y')$. Using $\gamma_K^{-1} = \gamma_K$,

$$U(x, y) = U'(-x, y)$$

Choosing $\mathbf{k}$ in the x-direction $\mathbf{k}\cdot\mathbf{x}' = -\mathbf{k}\cdot\mathbf{x}$, the envelope terms in the reflected coordinate system is written as

$$\begin{aligned} U'(\mathbf{x}') &= A'(\mathbf{x}')\, e^{i\mathbf{k}\cdot\mathbf{x}'} + A^{*\prime}(\mathbf{x}')\, e^{-i\mathbf{k}\cdot\mathbf{x}'} \\ &= A'(\mathbf{x}')\, e^{-i\mathbf{k}\cdot\mathbf{x}} + A^{*\prime}(\mathbf{x}')\, e^{i\mathbf{k}\cdot\mathbf{x}} \end{aligned}$$

the effect of the reflection is

$$A'(\mathbf{x}') = A^*(\mathbf{x}) \tag{4}$$

(c) Rotation. Rotating a pattern consists of the application of a two dimensional action $\gamma_R \in R$, where

$$\gamma_R = \begin{pmatrix} \cos\theta & \sin\theta \\ -\sin\theta & \cos\theta \end{pmatrix}$$

The equivariance gives

$$\begin{aligned} U'(\mathbf{x}') &= U'(\gamma_R^{-1}\mathbf{x}) \\ U'(\mathbf{x}') &= A'(\mathbf{x}')\, e^{i\mathbf{k}\cdot\mathbf{x}'} + A^{*\prime}(\mathbf{x}')\, e^{-i\mathbf{k}\cdot\mathbf{x}'} \\ &= A'(\mathbf{x}')\, e^{i\mathbf{k}'\cdot\mathbf{x}} + A^{*\prime}(\mathbf{x}')\, e^{-i\mathbf{k}'\cdot\mathbf{x}} \end{aligned} \tag{5}$$

Matching terms in Eqs. (1) and (5), $A(\mathbf{x})\, e^{i\mathbf{k}\cdot\mathbf{x}} = A'(\mathbf{x}')\, e^{i\mathbf{k}'\cdot\mathbf{x}}$. Thus

$$A'(\mathbf{x}') = A(\mathbf{x})\, e^{i(\mathbf{k}-\mathbf{k}')\cdot\mathbf{x}} \tag{6}$$

Rotation thereby modifies the envelope by a position-dependent phase.

2.3. Derivation of δ

In this section, we derive the structure of an operator $\odot$ such that $\odot A$ is equivariant under all rigid motions of a labyrinthine pattern. We will write $\odot = \odot(\alpha, \partial_x, \partial_y)$, where α denotes the derivative-independent parts of $\odot$. Since stripes have a constant envelope and the disorder parameter for stripes is zero by definition, then

$$\odot A(x) = \odot(\alpha, \partial_x, \partial_y)\, a_0 = \alpha a_0 = 0$$

Since $a_0 \neq 0$ in general, α must be zero, and the operator $\odot$ can be written as $\odot = \odot(\partial_x, \partial_y)$, (or $\odot' = \odot'(\partial_x, \partial_y)$ in a second coordinate system). Next, we deduce the implications on the form of $\odot$ imposed by the equivariance of $\odot A$ under rigid motions.

1. Invariance under Translation. Under translations

$$\odot' A'(\mathbf{x}') = [\odot'(\partial_x, \partial_y)](A(\mathbf{x})\, e^{i\mathbf{k}\cdot\mathbf{x}_t}) = [\odot A(\mathbf{x})]\, e^{i\mathbf{k}\cdot\mathbf{x}_t}$$

in accordance with Eq. (3).

$$|\odot' A'(\mathbf{x}')| = |\odot A(\mathbf{x})|$$

An invariant measure is obtained by considering $|\odot A(\mathbf{x})|$. Since $A \to \bar{A}$ under a reflection (about the y-axis) this choice leaves the disorder equivariant under reflections.

2. Invariance under Rotation. Equivariance under rotation of the field $A(\mathbf{x})$

$$e^{i(\mathbf{k}-\mathbf{k}')\cdot\mathbf{x}}[\odot A(\mathbf{x})] = \odot'(\partial_x, \partial_y)(A'(\mathbf{x}')) \\ = \odot'(\partial_x, \partial_y)(A(\mathbf{x})\, e^{i(\mathbf{k}-\mathbf{k}')\cdot\mathbf{x}}) \tag{7}$$

We use the requirements that perfect stripes have no disorder to determine one form for the circle operator, $\odot$. The left-hand side of Eq. (7) must be zero for perfect stripes because the envelope function is a constant, $(A(\mathbf{x}) = a_0)$. Equation (7) then reduces to

$$[\odot'(\partial_x, \partial_y)]\, e^{i(\mathbf{k}-\mathbf{k}')\cdot\mathbf{x}} = 0 \tag{8}$$

The actions of the derivatives on the exponential gives

$$\odot(\partial_x, \partial_y)\, e^{i(\mathbf{k}-\mathbf{k}')\cdot\mathbf{x}} = \odot(ik(1-\cos\theta), ik\sin\theta)\, e^{i(\mathbf{k}-\mathbf{k}')\cdot\mathbf{x}} = 0$$

Since $e^{i(\mathbf{k}-\mathbf{k}')\cdot\mathbf{x}}$ is not equal to zero, its prefactor must vanish. The lowest-order independent factor involving sines and cosines which equals zero identically is $\cos^2\theta + \sin^2\theta - 1$, so this term should be a factor of $\odot(ik(1-\cos\theta), ik\sin\theta)$ It is easily seen that this factor corresponds to the operator

$$\odot = \vec{k}\cdot\nabla - \frac{i}{2}\nabla^2 \tag{9}$$

The "local" deviations of the pattern from perfect stripes $|\odot A|$ can be integrated to give the disorder parameter, δ for a pattern.

$$\delta = \frac{\iint |\odot A(x)|\, da}{k_0^2 \langle |A(x)| \rangle} \tag{10}$$

The disorder has been normalized so that the intensive variable $\bar{\delta}$ is scale invariant.

2.4. Form of Higher Order Operators

The form of $\odot$ was deduced by imposing the equivariance of $\odot A$ under all rigid motions. It was the lowest order (in derivatives) that satisfies this property. In this section, we show that any operator $\square(\partial_x, \partial_y)$

such that $\Box A$ is equivariant is a polynomial of $\odot$. As before, the equivariance of $\Box A$ implies that

$$e^{i(\mathbf{k}-\mathbf{k}')\cdot\mathbf{x}}\Box A = \Box' A'(x') = \Box'(A(x)\, e^{i(\mathbf{k}-\mathbf{k}')\cdot\mathbf{x}}) \tag{11}$$

The argument of the last subsection (with $A = \text{const.} = a_0$) implies that $\odot$ is a factor of $\Box$. Write $\Box = \odot(\alpha_1 + \Delta_1)$ where α_1 is a constant, and Δ_1 contains the terms with derivatives ∂_x and ∂_y. To determine the form of Δ_1, substitute $A(x) = x$. Equation (11) gives

$$e^{i(\mathbf{k}-\mathbf{k}')\cdot\mathbf{x}}\Box x = \Box'(xe^{i(\mathbf{k}-\mathbf{k}')\cdot\mathbf{x}})$$

Using $\Box = \odot(\alpha_1 + \Delta_1)$, $\Box' = \odot'(\alpha_1 + \Delta_1')$ and using $\odot'(xe^{i(\mathbf{k}-\mathbf{k}')\cdot\mathbf{x}}) = (\odot x)\, e^{i(\mathbf{k}-\mathbf{k}')\cdot\mathbf{x}}$, it is seen that $\alpha_1 = \alpha_1'$ and

$$\Delta' e^{i(\mathbf{k}-\mathbf{k}')\cdot\mathbf{x}} = 0$$

thus $\odot' \mid \Delta_1'$ (i.e., $\odot'$ is a factor of Δ'), and similarly $\odot \mid \Delta_1$. Thus $\Delta_1 = \odot(\alpha_2 + \odot\Delta_2)$.

This process can be continued. We complete the result inductively. Suppose

$$\Box = \sum_{j=0}^{j=n} \alpha_j \odot^j + \odot^n \Delta_n$$

where Δ_n contains terms with derivatives ∂_x and ∂_y. Substituting $A(x) = x^n$ gives

$$e^{i(\mathbf{k}-\mathbf{k}')\cdot\mathbf{x}}(\Box x^n) = \Box'(x^n e^{i(\mathbf{k}-\mathbf{k}')\cdot\mathbf{x}})$$

$$e^{i(\mathbf{k}-\mathbf{k}')\cdot\mathbf{x}}\left(\sum_{j=0}^{j=n} \alpha_j \odot^j + \Delta_n \odot^n\right)(x^n) = \left(\sum_{j=0}^{j=n} \alpha_j \odot^j + \Delta_n \odot^n\right)'(x^n e^{i(\mathbf{k}-\mathbf{k}')\cdot\mathbf{x}})$$

$$e^{i(\mathbf{k}-\mathbf{k}')\cdot\mathbf{x}}(\Delta_n \odot^n)(x^n) = (\Delta_n' \odot'^n)(x^n e^{i(\mathbf{k}-\mathbf{k}')\cdot\mathbf{x}})$$

Using Eq. (7) n times on the right hand side for $\odot$ yields

$$e^{i(\mathbf{k}-\mathbf{k}')\cdot\mathbf{x}}(\Delta_n)(\odot^n x^n) = \Delta_n'[e^{i(\mathbf{k}-\mathbf{k}')\cdot\mathbf{x}}(\odot^n x^n)]$$

$$0 = \Delta_n'[e^{i(\mathbf{k}-\mathbf{k}')\cdot\mathbf{x}}]$$

Hence $\odot \mid \Delta_n$, and the result stated at the beginning of this subsection is proven.

3. CALIBRATING THE DISORDER PARAMETER

We evaluate the disorder parameter δ for several patterns whose analytical form is known These results will be used to confirm the validity of the numerical methods presented in the next section and to estimate their errors.

3.1. Stripes

The disorder parameter for a striped array of fixed width is $\delta = 0$. This condition holds for any orientation. We test our programs with data sets of stripes oriented at different angles from 0° to 180°, by angular differences of 10°.

Using stripes, we can also demonstrate the sensitivity of δ towards the correct value of k_0. Using an incorrect value, k, can increase the value of δ. To show this, we expand a perfect set of stripes with characteristic wavelength k_0 along a lattice base on a wave vector with a different magnitude k. Then we take the circle operator in the new basis. If the pattern is given by $e^{ik_0 x}$, then the misaligned envelope is $e^{i(k_0-k)x}$, and the operation gives

$$\left(k\frac{\partial}{\partial x}-\frac{i}{2}\nabla^2\right)e^{i(k_0-k)x}=k[i(k_0-k)]-\frac{i}{2}[i(k_0-k)]^2$$

$$=\frac{i}{2}k_0^2-\frac{i}{2}k^2$$

$$=i\frac{1}{2}(k_0+k)(k_0-k)$$

Hence $\bar{\delta}=|k^2-k_0^2|$. Thus, in estimating δ, we should take care to use the best possible value of k_0.

3.2. Target Pattern

A steady, circularly symmetric, target pattern is particularly useful for analysis because it is a non-trivial pattern whose disorder parameter can be calculated exactly. The equation for a target pattern is

$$U(\mathbf{x})=a_0e^{ikr}=a_0e^{ik\sqrt{x^2+y^2}}$$

Expanding as before gives

$$u(\mathbf{x}) = a_0 e^{i\mathbf{k}\cdot\mathbf{r}} = a_0 e^{i\mathbf{k}\cdot(\mathbf{r}-\mathbf{x})} e^{i\mathbf{k}\cdot\mathbf{x}}$$

Therefore $A'(\mathbf{x}') = a_0 e^{i\mathbf{k}\cdot(\mathbf{r}-\mathbf{x})}$. Thus,

$$\begin{aligned}\odot' A'(\mathbf{x}') &= \left(k\frac{\partial}{\partial x} - \frac{i}{2}\nabla^2\right)(a_0 e^{i\mathbf{k}\cdot(\mathbf{r}-\mathbf{x})}) \\ &= a_0\left\{k\left(\frac{ikx}{r} - ik\right) - \frac{i}{2}\left[\frac{ik}{r} - 2k^2\left(1 - \frac{x}{r}\right)\right]\right\} e^{i\mathbf{k}\cdot(\mathbf{r}-\mathbf{x})} \\ &= a_0\left\{\frac{k}{2r}\right\} e^{i\mathbf{k}\cdot(\mathbf{r}-\mathbf{x})}\end{aligned}$$

For the target pattern, the value of δ depends on the shape of the domain. If we integrate over a circular domain of radius R, the disorder parameter is

$$\delta = \frac{\int_0^{2\pi}\int_0^R |\odot A'|\, r\, dr\, d\theta}{k^2\langle |A'| \rangle} = \frac{\int_0^{2\pi}\int_0^R (a_0 k/2r)\, r\, dr\, d\theta}{k^2 a_0} = \frac{\pi R}{k}$$

However, typical data sets occupy a square domain, not a circular one. Therefore, the limits of integration are different.

$$\delta = \frac{\int_{-L/2}^{L/2}\int_{-L/2}^{L/2} [(a_0 k)/(2\sqrt{x^2+y^2})]\, dx\, dy}{k^2\langle |a_0| \rangle}$$

Substituting $x = y \sinh t$ into the integration over the x-coordinate reduces the integral to

$$\delta = \frac{a_0 k \int_{-L/2}^{L/2} \sinh^{-1}(L/y)\, dy}{k^2\langle |a_0| \rangle}$$

Another substitution, using $t = y/L$, yields an integral that can be found numerically. The resulting disorder parameter for a target pattern in a square domain is of side L is

$$\delta = 1.7627\frac{L}{k}$$

3.3. Domain walls

Domain walls are boundaries between one striped region and another. They can be described by the angle at which the stripes intersect and the width over which the transition from one orientation to the next occurs. If $\theta = 0$, then the stripes are parallel and the domain wall is trivial. Therefore, for $\theta = 0$, we should have $\delta = 0$.

In Fig. 2, stripes are oriented at $\theta = \theta_0$ in the top half of the picture and switch to $\theta = -\theta_0$ in the bottom half. The angle changes across the boundary roughly by the equation $\theta = \theta_0 \tanh((y - y_0)/w)$, where y_0 is the middle of the domain wall, and w adjusts its severity. The wave vector is written as $\vec{k} = k\cos\theta\hat{\imath} + k\sin\theta\hat{\jmath} = k\cos\theta(\hat{\imath} + \tan\theta\hat{\jmath})$. If we maintain a constant value of k_x, then $k\cos\theta = k_0\cos\theta_0$ at all points. Thus the formula for the wave vector is

$$\vec{k} = k_0\cos\theta_0\left[\hat{\imath} + \tan\left(\theta_0\tanh\left(\frac{y - y_0}{w}\right)\right)\hat{\jmath}\right]$$

This is a very complicated expression which causes many complications when it appears in the exponential term $e^{i\mathbf{k}\cdot\mathbf{x}}$. The operator $\odot$ adds to the confusion. We can however check the disorder parameter at small angles using the small angle approximation. First we can set $y_0 = 0$. Then

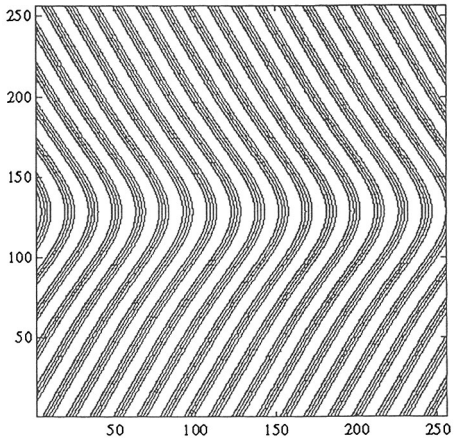

Fig. 2. A domain wall between two regions of stripes with different orientations. The disorder parameter δ is a monotonically increasing function of the angle between the stripes.

for small angles $\tanh x \cong x - x^2$, and $\tan\theta \cong \theta$. The wave vector simplifies to

$$\vec{k} = k_0 \cos\theta_0 \left[\hat{\imath} + \theta_0 \left(\frac{y}{w} - \frac{y^2}{w^2} \right) \hat{\jmath} \right]$$

When this linearization is used in the exponential term,

$$\odot A = \left[\begin{array}{l} ik_0(\cos\theta_0 - 1) - \dfrac{i}{2}\left[-k_0^2(\cos\theta_0 - 1)^2 - k_0\theta_0 \cos^2\theta_0 \left(\dfrac{4y^2}{w^2} \right) \right] \\ \qquad + ik_0\theta_0 \cos\theta_0 \left(\dfrac{2}{w} - \dfrac{6y}{w} \right) \end{array} \right] e^{i\phi}$$

where $\phi = k_0(\cos\theta_0 - 1)\, x + k_0\theta_0 \cos\theta_0 (y^2/w - y^3/w^2)$. The disorder parameter can be computed by integrating over the entire domain numerically. As expected, $\delta_{\theta=0} = 0$ and δ increases as the angle between the two striped domains increase. This alone is information that cannot be obtained by other methods such as the correlation length and spectral entropy.

4. NUMERICAL EVALUATION OF δ FOR LABYRINTHINE PATTERNS

The Fast Fourier Transform can be used to determine the disorder parameter. Fourier analysis has the advantage of speed and precision when performing the derivatives required to evaluate $\odot A$.

Once we transform the pattern to Fourier space, an azimuthal averaging determines its average spatial frequency. Since we apply $\odot$ on the envelope of the pattern $A(\mathbf{x})$ rather than on the pattern $u(\mathbf{x})$ itself, we need to extract the transform $\hat{A}(\mathbf{k})$ of the complex envelope from the transform $\hat{u}(\mathbf{k})$ of the pattern. First, we create the spectrum for the corresponding complex pattern by deleting the half of the spectrum which lies to the $-k_x$ side of the origin and doubling the points which lie on the positive side. We choose these points because of an initial choice of vector which lies along the x-axis. Values lying on the k_y-axis are real-valued and are left alone. This procedure leaves us with only the complex pattern.

Once we have the complex pattern, we create the complex envelope by shifting the spectrum in the k_x direction by the average frequency of the pattern, since the relation in complex space $f(\mathbf{x}) = A(\mathbf{x})\, e^{ik_0 x}$ transforms to $\hat{f}(\mathbf{k}) = \hat{a}(\mathbf{k} - \mathbf{k_0})$. Once we obtain the transform of the complex envelope function, we are ready to perform the derivatives required to get $\odot A$. A spatial derivative $\partial A/\partial x$ transforms to a scalar multiplication, $ik_x \hat{A}(\mathbf{k})$,

in Fourier space. The whole circle operation therefore becomes a process of multiplying the intensity peaks at each frequency by the appropriate scalar and correctly summing the results.

5. AN APPLICATION: RELAXATION OF PATTERNS

In this section, we present results from the integration of the Gray–Scott Model, which demonstrate configuration-independent features of the relaxation of patterns.

5.1. Gray–Scott Model

The Gray–Scott model is the following pair of reaction-diffusion equations.[2]

$$A + 2B \rightarrow 3B$$

$$B \rightarrow C$$

They are based on a more complex set of chemical reactions derived from biological systems. Three rates determine the total reaction rates of chemicals A and B: the individual chemical reaction rates, the diffusion rates, and the rates at which these chemicals are fed into the system. With suitable normalizations, the evolution of $a = [A]$ and $b = [B]$ can be modeled by

$$\frac{da}{dt} = D_1 \nabla^2 a - ab^2 + F(1-a)$$

$$\frac{db}{dt} = D_2 \nabla^2 b + ab^2 - (F+k)\, b$$

D_1 and D_2 are the diffusion rates of A and B respectively, F is a dimensionless feed rate and k is the dimensionless rate constant for the second reaction. We follow the experimental setup outlined by Pearson[17] and choose $D_1 = 2 \times 10^{-5}$, and $D_2 = 10^{-5}$.

The stationary solutions to these equations are the trivial state, $(\bar{a}, \bar{b}) = (1, 0)$ and the solutions

$$(\bar{a}_1, \bar{b}_1) = \left(\frac{1}{2F} [F + \sqrt{\Delta}], \frac{1}{2(F+k)} [F - \sqrt{\Delta}] \right)$$

$$(\bar{a}_2, \bar{b}_2) = \left(\frac{1}{2F} [F - \sqrt{\Delta}], \frac{1}{2(F+k)} [F + \sqrt{\Delta}] \right)$$

where $\Delta = F^2 - 4F(F+k)^2$. In order for these solutions to be real numbers, the discriminant must be positive ($F^2 - 4F(F+k)^2 \geqslant 0$). Solving for the equality determines the boundary between regions of real and complex solutions, which is

$$F = 0, \qquad (\tfrac{1}{8})[(1-8k) \mp \sqrt{1-16k}] \tag{12}$$

The solution to Eq. (12) is the solid curve in Fig. 4. The region between the curves supports two real solutions to the Gray–Scott equations. Outside of this region there are no real solutions. Along this curve, the only nontrivial solution is $(a, b) = (0.25, \sqrt{F})$.

Linear stability analysis determines the conditions at which patterns will appear. Representing a small perturbation around the stable point with $(a, b) = (\bar{a} + \delta a, \bar{b} + \delta b)$, and assuming $\delta a = \tilde{a} \exp\{i\mathbf{s} \cdot \mathbf{r} + \omega t\}$, $\delta b = \tilde{b} \exp\{i\mathbf{s} \cdot \mathbf{r} + \omega t\}$, we find a Hopf bifurcation along the following curve:

$$(F+k)^4 = F^2 k \tag{13}$$

Pearson[17] has mapped the types of patterns which form at given parameter values. He discovered several regions of striped behavior, several with hexagonal structure, and some turbulent regions. Our methods for producing these patterns were taken from his paper with developmental help from Valerie Petrov at the University of Texas at Austin.

5.2. Initial Setup

Pearson initializes his entire domain to the trivial state ($a = 1, b = 0$) except for a small region at the center where he sets initial values to $(a, b) = (\frac{1}{2}, \frac{1}{4}) + \textit{noise}$. Patterns form at the moving boundary between the trivial state and the seeded region, and the noise breaks the square symmetry of the pattern. Although this method works successfully at all relevant parameter values, patterns formed by this method do not cover the entire region until approximately 10,000 time steps, at which time the patterns become static. We are interested in characterizing the evolution of a pattern which appears all at once over the entire domain. Since we cannot calculate a definite value of the frequency until the pattern extends throughout the region, we need to seed the entire region.

In order to form patterns globally and quickly, we need to seed the entire data set, not just a small region. Unfortunately, seeding the entire domain requires caution. In the region of parameter space where no real solutions exist, a domain seeded with random numbers quickly decays to the trivial state. In order to produce non-trivial patterns in this region, we must correlate the initial values of each pixel with its neighbor. We do this

by studying the final state of patterns evolved by Pearson's method. Upon examination, final values of a range approximately from 0.3 to 0.8, while final values for b typically range from 0 to 0.3. With this in mind, we limit our initial conditions to lie within these ranges. To further control our seeding process, the initial value at any point is the average of previously-seeded nearest neighbors plus some random noise. This reduces local randomness and stresses continuity of values between points, thereby reducing the initial strength of the diffusion term. The first point (top left corner) is seeded at (0.5, 0.25). Noise levels set are at 50%.

For all realizations, data is recorded at $t = 125$, 250, 500, 1000, 2000, 4000, 8000, 16000, and 32000 time steps. We used the Bulirsch–Stoer method,[18] with each time step equal to 1 second. After 32000 time steps, the time between recorded data sets gets prohibitively long, whereas the patterns do not change noticeably over this time scale. The simulation was run on a DEC Alpha at 200 MHz with a grid size of 256×256.

5.3. Evolution of the Disorder Parameter

Figures 3a and 3b show two realizations of the Gray–Scott model at the parameter values $k = 0.06$ and $F = 0.042$. Since these external parameters are the same for each, the resulting patterns share common features. Differences in the initial conditions of each realization cause each pattern inevitably to be unique. Despite these initial conditions and the differences between the details of the patterns at any given moment, the patterns evolve in a similar fashion and at the same rate. In both cases, the complete pattern is apparent in its entire form only at $t \cong 1000$ seconds. Before this, the stripes do not occupy the entire space. After 1000 seconds, the patterns change very little but their features sharpen.

For our experiment, we ran the Gray–Scott model at several parameter values. Figure 4 shows a close-up of the parameter space The solid curve separates the real and imaginary solutions and the dotted curve represents the point of the Hopf bifurcation. At each designated point in parameter space, we ran four realizations under different initial conditions. Then we calculated the disorder parameter at each of the recorded time steps in each realization. We plotted the disorder parameter vs. time for each realization at the designated values of F and k, and calculated the slopes by visually determining the average values of the disorder parameter.

The results are best viewed when plotted as δ vs. $\log(t)$ as shown in Fig. 5. The close agreement between the curves of each graph indicates that δ is indeed independent of the individual configurations (i.e., initial conditions) of the pattern at all times. This result is in good agreement with the patterns of Fig. 3, which are very similar, despite being unique.

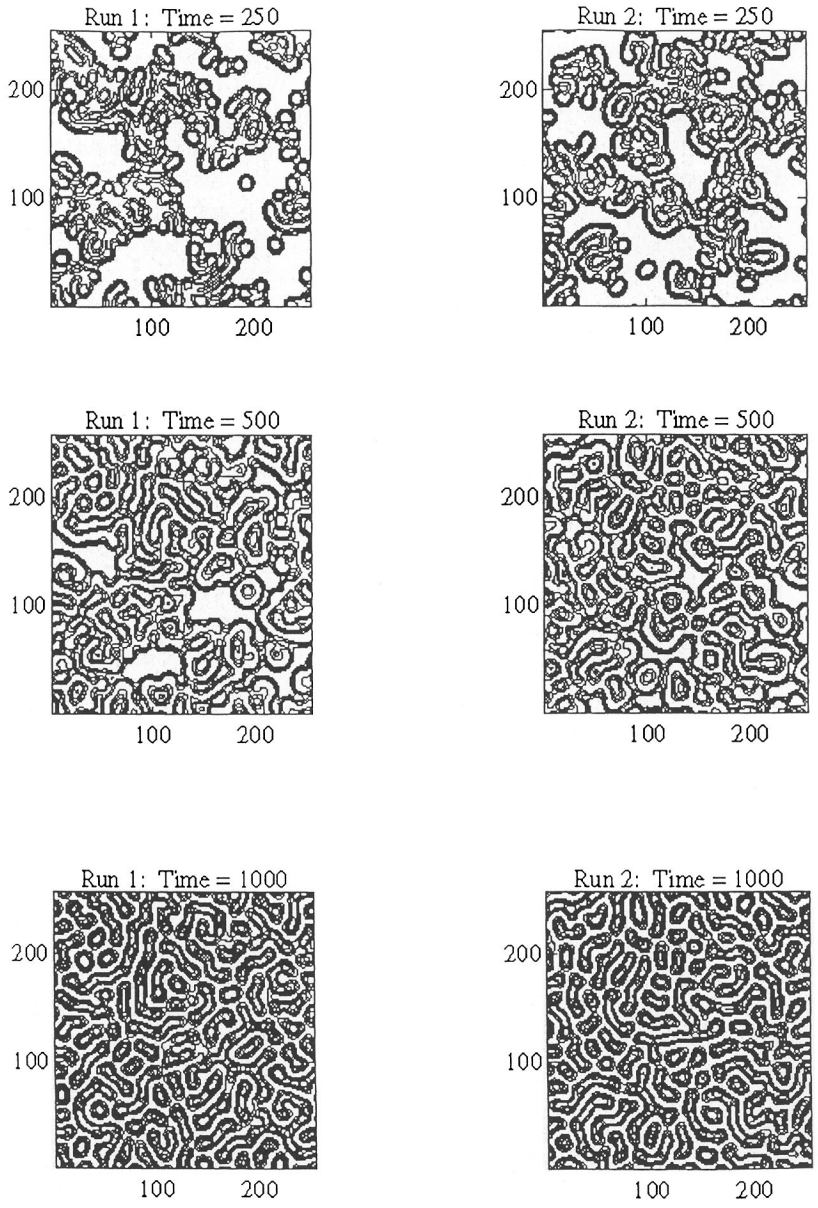

Fig. 3. The generation of labyrinthine patterns from random initial states. The details of snapshots from the two runs shown are different at each stage. However, the presence of common characteristics at each stage of the evolution is easily observed.

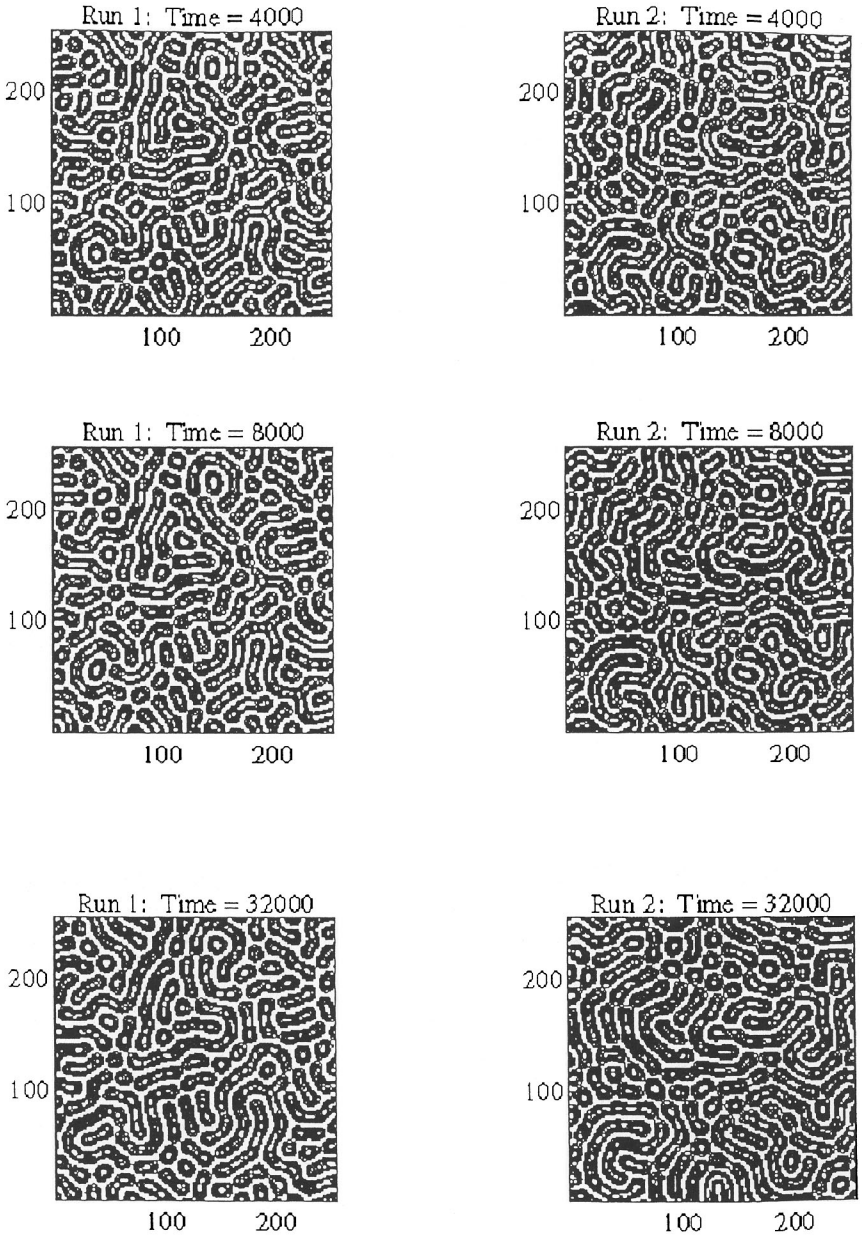

Fig. 3. (*Continued*)

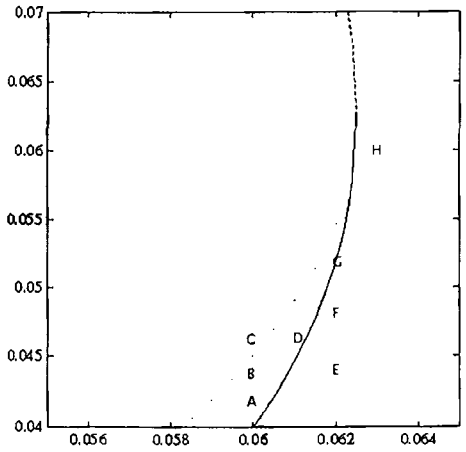

Fig. 4. Closeup of the parameter space of the Gray–Scott model with representative points labeled (see Table I).

The differences in the shapes of the decay curves between graphs indicates that δ depends on the external parameters of the experiments. This is again in good agreement with the patterns which from at each new set of parameters. Changing these parameters changes crucial characteristics such as the density of point defects and the severity of domain walls. These new features are reflected in the decay rate of the disorder parameter.

Table I. The Two Distinct Slopes of the Curve $\log(t)$ vs. $\delta(t)$ for Several Parameter Values of The Gray–Scott Model[a]

Letter	k	F	slope1	slope2
A	0.06	0.042	−0.0719	−0.0063
B	0.06	0.044	−0.1019	−0.0042
C	0.06	0.046	−0.0481	−0.0084
D	0.061	0.046	−0.0491	−0.0086
E	0.062	0.044	−0.0915	−0.0049
F	0.062	0.048	−0.0322	−0.0071
G	0.063	0.052	−0.0347	−0.0048
H	0.063	0.06	−0.0451	−0.0100

[a] The points *A*, *B*, etc. are those shown in Fig. 4. "slope1" refers to the initial value of the slope and "slope2" refers to the value after transition.

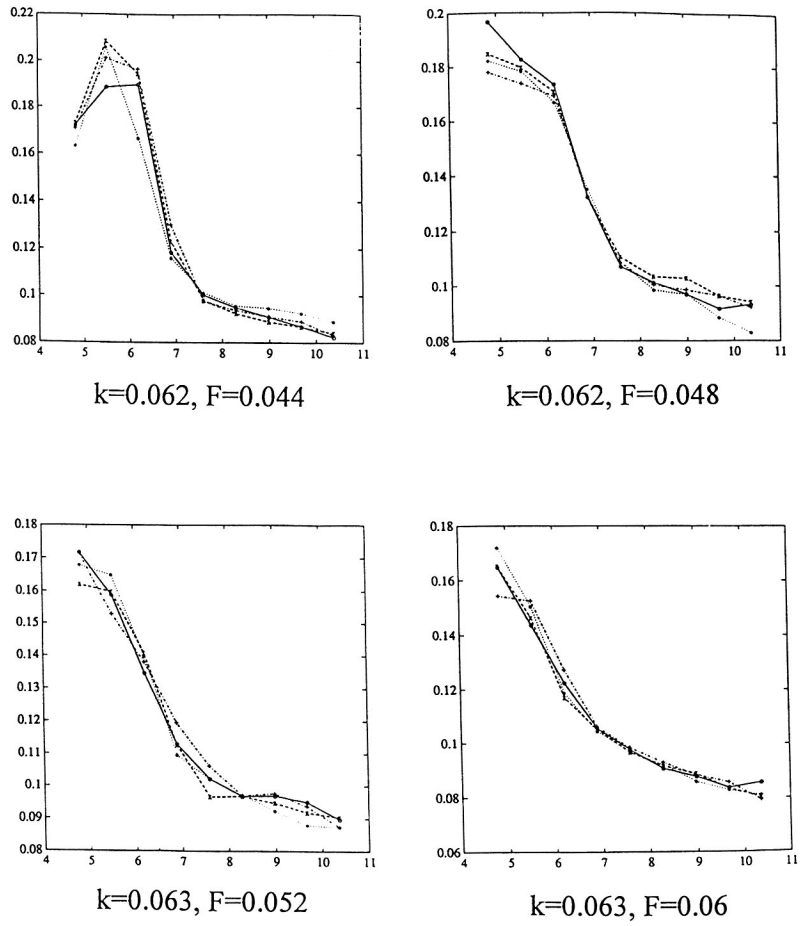

Fig. 5. The behavior of δ as a function of (the logarithm of) time for multiple runs at several values of the control parameters. For given control parameters, the curves $\delta(t)$ are configuration independent. Furthermore, the time evolution of the disorder parameter consists of two phases, each with logarithmic decay of δ. The decay rates are parameter dependent.

5.4. Behavior of $\delta(t)$

The disorder parameter shows that the Gray–Scott model decays to an ordered state. Each curve displays two distinguishable rates of decay. The first rate is due to the relaxation of the data out of the initial disordered state. Once the pattern has formed, it relaxes into a final state, causing the slower rate found at the later times. The values of these slopes are displayed against the parameters F and k in Table I.

For early time steps, (~ 100 seconds) poor values of k_0 can cause bizarre behavior of the disorder parameter, as in graphs for $k = 0.06$, $F = 0.042$ and $k = 0.06$, $F = 0.044$. Once the fundamental frequency is well-established, a better reading of the disorder parameter is possible. The character of the decay in the disorder parameter is tied to the external parameters (seen in the shapes of the curves of Fig. 5) rather than to the specific initial conditions (note the semblance among curves at the same external parameters). We therefore see a universal property of the decay rate in the Gray–Scott model equations.

6. CONCLUSIONS

The form of the disorder parameter δ was derived by imposing its equivariance under all rigid motions of a single pattern. Rather surprisingly, it was found that δ is the same for multiple configurations generated under identical external conditions; i.e., it is a configuration independent characterization of labyrinthine patterns. In addition, analysis of patterns generated in experiments and model systems show that δ is an extensive variable. The corresponding *intensive variable* $\bar{\delta} = \delta/(Area)$ can be used to compare and contrast distinct patterns. In particular $\bar{\delta}$ can be used to contrast patterns with visually different characteristics.[9]

Patterns generated in experiments (e.g., Faraday experiment in a granular layer[12]) show the organization (in time) of an initially random state to the final labyrinthine structure. We have analyzed similar behavior in patterns generated in a model system, and have shown that the disorder parameter captures configuration independent properties of the relaxation. The evolution of initially random states exhibits two distinct phases, each accompanied by a logarithmic decay of δ. (This behavior is reminiscent of the relaxation in the decay of the Flux Creep in "hard" superconductors.[13, 14]) During the first phase the random initial state develops into small independent striped domains. During the second phase, the domains compete with each other for dominance. The presence of two distinct phases of the evolution (with a sharp transition) is clearly seen in the behavior of $\bar{\delta}(t)$.

Analysis of experimental patterns has one additional complication. These structures (unlike patterns generated in model systems) do not have periodic boundary conditions. The spectral methods used to evaluate δ (Section 4) can be applied to data that are modified by tapering the original data near the boundaries (e.g., with Gaussian functions) so that the field vanishes at the boundaries. The modified fields are periodic, and methods discussed in Section 4 can be implemented. Preliminary analysis of experimental patterns demonstrate behavior in $\bar{\delta}(t)$ that is similar to the results discussed in Section 5.

ACKNOWLEDGMENTS

We have benefited from discussions with M. Field, M. Golubitsky, M. Gorman, I. Melbourne, H. L. Swinney and P. Umbanhower. This research is supported by the Office of Naval Research and the Energy Laboratory of the University of Houston.

REFERENCES

1. J. Murray, *Mathematical Biology*, Biomathematics Texts (Springer-Verlag, Berlin, 1989).
2. P. Gray and S. K. Scott, Autocatalytic reactions in the isothermal, continuous stirred tank reactor, isolas and other forms of multistability, *Chem. Eng. Sci.* **38**:29 (1983); P. Gray and S. K. Scott, Sustained oscillations and other exotic patterns of behavior in isothermal reactions, *J. Phys. Chem.* **89**:22 (1985).
3. M. C. Cross and P. C. Hohenberg, Pattern formation outside of equilibrium, *Rev. Mod. Phys.* **65**:(1993) 851.
4. Q. Ouyang and H. L. Swinney, Transitions to chemical turbulence, *Chaos* **1**:411–420 (1991).
5. M. C. Cross and D. I. Meiron, Domain coarsening in systems far from equilibrium, *Phys. Rev. Lett.* **75**:2152 (1995).
6. D. A. Egolf, I. V. Melnikov, and E. Bodenschatz, A new fast method for determining local properties of striped patterns, submitted to *Nature*.
7. K. R. Elder, J. Viñals, and M. Grant, Ordering dynamics in the two-dimensional stochastic Swift–Hohenberg equation, *Phys. Rev. Lett.* **68**:3024 (1992).
8. D. A. Egolf and H. S. Greenside, Characterization of the transition from defect to phase turbulence, *Phys. Rev. Lett.* **74**:1751 (1995).
9. G. H. Gunaratne, R. E. Jones, Q. Ouyang, and H. L. Swinney, An invariant measure of disorder in patterns, *Phys. Rev. Lett.* **75**:3281 (1995).
10. M. Golubitsky, I. Stewart, and D. Schaeffer, *Singularities and Groups in Bifurcation Theory*, Vol. 2. Appl. Math. Sci. 69 (Springer, New York, 1988).
11. A. Newell and J. Whitehead, Finite bandwidth, finite amplitude convection, *J. Fluid Mech.* **38**:279 (1969).
12. F. Melo, P. Umbanhower, and H. L. Swinney, Transition to parametric wave patterns in a vertically oscillated granular layer, *Phys. Rev. Lett.* **72**:172 (1993).
13. P. W. Anderson and Y. B. Kim, Hard superconductivity: Theory of the motion of Abrikosov flux lines, *Rev. Mod. Phys.* **36**:39 (1964).
14. C. Tang, SOC and the Bean critical state, *Physica A* **194**:315 (1993).
15. G. H. Gunaratne, A Theory of Patterns, *Chaos, Solitons & Fractals* **5**:1447 (1995).
16. P. Manneville, *Dissipative Structures and Weak Turbulence* (Academic Press, Boston, 1990).
17. J. E. Pearson, Complex patterns in a simple system, *Science* **261**:189 (1993).
18. W. H. Press, S. A. Teukolsky, W. T. Vetterling, and B. P. Flannery, *Numerical Recipes in C: The Art of Scientific Computing*, 2nd ed. (Cambridge University Press, Cambridge, 1992).
19. L. A. Segel, Distant side-walls cause slow amplitude modulation of cellular convection, *J. Fluid Mech.* **38**:203 (1969).
20. A. M. Turing, The chemical basis of morphogenesis, *Phil. Trans. R. Soc. London B* **37**:37 (1952).